Journal Pre-proofs

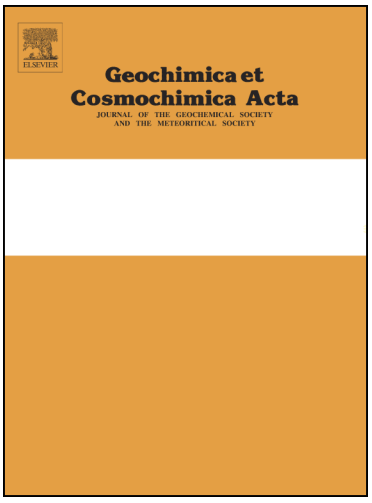

Diffusion of noble gases in subduction zone hydrous minerals

Kai Wang, Xiancai Lu, John P. Brodholt

PII: S0016-7037(20)30435-X
DOI: https://doi.org/10.1016/j.gca.2020.07.015
Reference: GCA 11841

To appear in: *Geochimica et Cosmochimica Acta*

Received Date: 7 December 2019
Revised Date: 21 June 2020
Accepted Date: 7 July 2020

Please cite this article as: Wang, K., Lu, X., Brodholt, J.P., Diffusion of noble gases in subduction zone hydrous minerals, *Geochimica et Cosmochimica Acta* (2020), doi: https://doi.org/10.1016/j.gca.2020.07.015

Diffusion of noble gases in subduction zone hydrous minerals

Kai Wang[1,*], Xiancai Lu[1,*], John P. Brodholt[2, 3]

1. State Key Laboratory for Mineral Deposit Research, School of Earth Sciences and Engineering, Nanjing University, Nanjing Jiangsu, 210026, China.
2. Department of Earth Sciences, University of College London, London WC1E 6BT, UK.
3. Centre for Earth Evolution and Dynamics (CEED), University of Oslo, 0316 Oslo, Norway.

Correspondence regarding this manuscript should be sent to Dr. Kai Wang and Prof. Xiancai Lu at the address of State Key Laboratory for Mineral Deposits Research, School of Earth Sciences and Engineering, Nanjing University, 163 Xianlin Road, Nanjing 210023, China.
E-mail: wangkaies@nju.edu.cn to Dr. Kai Wang, xcljun@nju.edu.cn to Prof. Xiancai Lu.
Fax: + 86-25-83594664

Abstract

Subduction of atmospheric noble gases has been considered to play an important role in altering the primordial isotopes of Earth's mantle over geological time. Analysis of natural samples and experiments indicate that large quantities of noble gases can be dissolved in volatile-bearing hydrous minerals in the subduction slabs. To quantitatively investigate the recycling efficiency of noble gases and relevant consequences on the mantle noble gas isotopic evolution, the diffusivities of noble gases in these minerals are needed. In this study, diffusion of He, Ne, Ar, Kr and Xe in lizardite, antigorite and tremolite have been calculated by first-principles methods based on density functional theory. Our results disclose that diffusion is slower with increasing radius of the noble gas atom ($D_{He} > D_{Ne} > D_{Ar} > D_{Kr} > D_{Xe}$) as expected. The common ring-structures in hydrous silicate minerals provide incorporation sites for the noble gas atoms and control their mobility. The diffusion activation energies are 84.9, 157.3, 287.5, 347.4, 414.9 kJ/mol from He to Xe in lizardite, and despite the very similar lattice structure between lizardite and antigorite, the activation energies are found to be significantly higher in antigorite, which are 120.6, 267.3, 449.6, 497.9 and 550.0 kJ/mol, respectively. In tremolite, the energy barriers are 93.6, 158.2, 266.3, 322.2 and 385.0 kJ/mol, which are also found to be in very good agreement with available experimental values and similar to those in lizardite. We also calculated diffusion activation energies at higher pressures (1 GPa for liazardite, 3 GPa for antigorite and tremolite) to better understand how much noble gases can be preserved against diffusive loss during subduction. Our result show that the oceanic crust and the

lithospheric mantle of the subduction slab play different roles in delivering noble gases into the mantle. We find that all Ar, Kr, Xe and possibly part of the Ne can be entrained by the serpentine-dominated lithospheric mantle into the deep mantle due to the high diffusive energy barriers in antigorite. In contrast, noble gases in the amphibole-enriched oceanic crust would be characterized by fractionated noble gas signature, with the concentrations of retained noble gases in the crust following their respective ionic radius (Ne < Ar < Kr < Xe).

1. Introduction

Due to their chemically inert nature and simple systematic behavior, the group of noble gas isotopes are ideal tools for tracing geological processes like mantle evolution and the origin the Earth's atmosphere (e.g. Farley et al., 1995; Graham, 2002; Trieloff and Kunz, 2005; Marty, 2012; Mukhopadhyay, 2012; Mukhopadhyay and Parai, 2019). Although it has been long known that subduction zones play a significant role in delivering volatile species, such as carbon, water, as well as other volatiles back to the Earth's interior (Staudacher and Allègre, 1988; Rüpke et al., 2004; Kendrick et al., 2011; Kendrick et al., 2013; Dallai et al., 2016; Kobayashi et al., 2017), the information regarding the recycling of noble gases still remains rather ambiguous and hampers the interpretation of the existence of air-like noble gas isotopic signatures in the mantle (Holland and Ballentine, 2006).

Previous studies demonstrated that subducting slabs consisting of oceanic sediments, altered oceanic crust and serpentinised mantle contain atmospheric noble gases that are 2 ~ 4 orders of magnitude more concentrated than in the ordinary depleted mantle (Staudacher and Allegre, 1988; Moreira et al., 2003; Kendrick et al., 2011). However, Staudacher and Allègre (1988) argued that the vast majority of subducted noble gases are transported back to the surface via arc volcanism caused by the dehydration of subducted hydrous minerals before they can reach deep mantle. This process is also known as the "subduction barrier" and is thought to strongly limit the ability of recycled material to affect noble gas concentrations and ratios in the mantle. But considering the Earth's mantle has been thoroughly degassed via surface magma activities, especially

through partial melting extraction of the underlying mantle at mid-ocean ridges, and that only ~ 1% or less of primordial noble gases remains in the mantle (Marty, 2012), any injection or regassing of the noble gases, even in small quantities, would still have significant influence on the mantle noble gas budget.

To better constrain the regassing contribution of the subduction process, it is critical to understand how much surface noble gases can be carried by subducting slabs and the dynamic behavior of noble gases during the subduction. The answer to the above questions depends on two fundamental parameters, the solubility of noble gas in the subduction zone minerals which determines the total budget in the slabs, and noble gas diffusion rates in relevant minerals that control their retentions, e.g. slow diffusion reduces the dehydration extraction of the noble gases from the minerals. Recent experiments have shown that the ring-site structure consisting of Si-O tetrahedra in the amphibole lattice – the dominant hydrous minerals in the altered oceanic crust – can readily accommodate abundant noble gases (Jackson et al., 2013). Further experiments confirm that high solubilities of noble gases is ubiquitous among hydrous minerals with ring-sites in their lattice structure (Jackson et al., 2015; Krantz et al., 2019).

While the solubilities of noble gases in ring-structure-bearing minerals are proving to be much higher than in other nominally anhydrous minerals in the mantle like olivine and pyroxene, studies on their diffusivities are still relatively scarce and only limited He, Ne and Ar diffusion data in amphiboles are available (e.g. Mark Harrison, 1982; Baldwin et al., 1990; Baxter, 2010; Jackson et al., 2016). The existing data indicates that the activation energies of diffusion for noble gases in amphibole are systematically

higher with increasing atom radius, i.e. 98.8 ~ 123.6 kJ/mol for He, 132.2 ~ 181.5 kJ/mol for Ne and 268.2 ± 7.1 kJ/mol for Ar. This range of diffusion activation energies suggests different subduction patterns for He, Ne and Ar. Light noble gases such as He and Ne have closure temperatures of 42 ~ 70 °C and 185 ~ 249 °C in amphibole respectively (assuming a cylinder mineral grain with 10 μm in radius, and 100 °C/Myr cooling rate, calculated according to Dodson, 1973), whereas the closure temperature is ~ 500 °C for Ar. Therefore, light noble gases will diffuse out of amphibole early while heavier ones will be still carried by the slabs. The diffusion or solubility controlled elemental fractionations among different noble gases during the subduction may, therefore, have significantly altered the mantle noble gas characteristics (Smye et al., 2017; Krantz et al., 2019).

Although amphibole is mainly responsible for the recycling efficiency of ocean crust, serpentinites are more important in hydrated lithospheric mantle (Bostock et al., 2002; Reynard, 2013). In natural samples, serpentine minerals are dominated by lizardite and antigorite. Lizardite is the main variety presents in low-grade serpentinites from the altered oceanic lithosphere and from low-grade metamorphic ophiolites (Evans, 2004; Zheng, 2019), whereas antigorite is the stable serpentine mineral in high-grade metamorphic phases (Ulmer and Trommsdorff, 1995). Thermodynamic data predict that above 300 °C, the antigorite + brucite assemblage is more stable than lizardite, and stability field of antigorite persists up to a ~ 650 °C at 3 GPa (Ulmer and Trommsdorff, 1995). These data indicate that serpentinites, especially those in cold subduction zones, can be subducted to depths well beyond the arc magma generation zone (e.g. Cai et al.,

2018).

In this study, atomic simulations based on density functional theory (DFT) were performed to study the diffusion of noble gases (He, Ne, Ar, Kr and Xe) both in serpentinites (lizardite and antigorite) and amphibole (tremolite). The effect of lattice structure of different ring-sites on the diffusion is also investigated and discussed. Based on the new diffusion data, together with the geological setting of subduction zones, we estimate the diffusive loss of noble gases from the mineral grains during subduction and discuss the possible fractionation of light (He, Ne) and heavy (Ar, Kr and Xe) noble gases entrained by the slabs.

2. Method

The diffusion coefficient D can be described following the Arrhenius form:

$$D = D_0 \exp(-\Delta E_a / k_B T) \qquad (1)$$

where ΔE_a is the activation energy, k_B is the Boltzmann constant, T is the temperature in Kelvin and D_0 is the pre-exponential factor. At atomic scale, D_0 is related to the jump distance l of the diffusive atom moving from one stable configuration to another, and the attempt frequency v that the diffusing atom tries to jump across the saddle point according to the harmonic transition state theory (Vineyard, 1957):

$$D_0 = \frac{1}{2} l^2 v \qquad (2)$$

The factor 1/2 is based on the fact that diffusion is usually directional dependent in anisotropic minerals, and calculations are performed with atoms moving in specific direction. The attempt frequency v can be further expressed as the ratio of lattice vibration frequencies when system in ground state or the diffusing atom is at the stable

site (v_i) to the frequencies when the atom is at the saddle point (v_i'):

$$v = \frac{\prod_{i}^{3N-3} v_i}{\prod_{i}^{3N-4} v_i'} \qquad (3)$$

where N is the number of atoms of the system studied.

In order to investigate all the necessary information involved in the diffusion processes, including the incorporation sites, the migration pathways, the energy barriers and the attempt frequencies, we have performed first principles calculations using density functional theory (DFT) implemented in the Vienna Ab-initio Simulation Package (VASP 5.4.1) (Kresse and Hafner, 1993; Kresse and Furthmüller, 1996). The projected augmented wave (PAW) method was used to describe the interactions between ions and electrons (Blöchl, 1994; Kresse, 1999), while the exchange and correlation energy between electrons was described by the generalized gradient approximation (GGA) of Perdew and Wang (PW91) (Perdew and Wang, 1992). The PAW parameters we used are extracted from VASP's library, where there are 2 valence electrons for Mg (s2p0), 4 for Si (s2p2), 6 for O (s2p4), 10 for Ca (3s3p4s), 1 for He (s1), 8 for Ne, Ar, Kr and Xe (s2p6) and ultrasoft pseudopotential for H.

In our earlier calculation we found a large supercell is necessary to get converged results on activation energy (Wang et al., 2015). In this study, we used 3 × 3 × 2 supercell (288 atoms) for lizardite, 1 × 1 × 2 supercell (582 atoms) for antigorite and 2 × 1 × 2 supercell (328 atoms) for tremolite. The Brillouin zone is sampled by a Monkhorst–Pack (Monkhorst and Pack, 1976) k-point grid with only gamma points due

to the large supercells employed here, and 500 eV energy cutoff for the plane-wave basis set is proven sufficient. The structures of the ideal minerals were first fully relaxed at target pressures by allowing both the lattice structure and the atom positions to be changed according to the conjugate gradient (CG) algorithm. The incorporation sites for noble gases were found by relaxing all the atom positions with 1 noble gas atom inserted in the possible interstitial sites. As the migration paths of noble gases in these minerals are usually not a simple direct jump, CI-NEB method has been employed to find the minimum energy migration pathways and the corresponding saddle points. The convergence threshold for structure relaxations was set as when the Hellmann-Feynman forces are smaller than 1×10^{-3} eV/Å. To calculate the atomic jump frequency, frequency calculations were performed by using the small displacements method implemented in the VTST scripts (http://theory.cm.utexas.edu/vtsttools/scripts.html) and the force convergence threshold was set below 1×10^{-7} eV/Å.

3. Calculation Results

The calculated lattice parameters of lizardite, antigorite and tremolite are given in Table 1 together with values from experiments and previous calculations. Our calculated results are consistent with previous studies, although the cell parameters are generally slightly larger than experiments. This is because the GGA method tends to underestimate chemical binding and thus leads to slightly larger volumes. Although lattice adjustment towards experimental values has been adopted in previous calculations (e.g. Zhang et al., 2013; Ghaderi et al., 2015), we do not apply it here since our previous study of helium diffusion in olivine without any adjustment achieved very

good agreement with experiments (Wang et al., 2015). Moreover, the difference in cell parameters between calculations and experiments in this case is very small.

3.1 Noble gas diffusion in lizardite

Serpentine minerals, which have the ideal formula $Mg_3Si_2O_5(OH)_4$, are made of superposed 1:1 alternating Si-O tetrahedral and Mg-(O-OH) octahedral sheets. The different spatial arrangements of these layers result in three main serpentine minerals, i.e., the sheets form flat layers in lizardite (e.g. Fig. 1), cylinders in chrysotile and corrugated modulated structures in antigorite (e.g. Fig. 2). Chrysotile is subordinate to lizardite in low-grade metamorphic facies (Evans, 2004; Schwartz et al., 2013), and its lattice structure is similar to that of the lizardite, so we performed the calculation only for lizardite and considered the results can also be applicable for chrysotile.

The tetrahedral sheets in lizardite are made of 6-membered rings of tetrahedra extending along *a*- and *b*-axis. The most stable configuration is when a noble gas atom sits at the center of the rings. Since the ring sites are all identical according the lattice symmetry, the diffusion along *a*- and *b*-axis is achieved by a noble gas atom moving from one ring to one of the six adjacent rings. The diffusion path is shown in Fig. 1., the 'S' shape of the path is because the atom has to navigate around the OH^- linked to the Mg-(O-OH) octahedral (OH^- are not shown in the figures for better illustration of the ring structure). However, to move in the *c* direction the atom has to cross over the close packed octahedral sheet and thus needs to overcome much higher energy barrier, i.e. the activation energy barrier for He moving in *a, b* direction is 84.9 kJ/mol compared to 301.0 kJ/mol in *c* direction. In this situation, the bulk diffusivity is totally

controlled by the lower activation energy process, and thus only diffusion along the *a,b-axis* for the other noble gases are calculated. Similar anisotropic structures also exist in antigorite and tremolite, and so in all cases the diffusion is dominated by the process of an atom moving in the interlayer space (lizardite and antigorite) or in the channel structure of tremolite.

3.2 Noble gas diffusion in antigorite

The bulk structure of antigorite has different variants characterized by the number of silicate tetrahedra, *m*, within one unit cell along the *a*-axis. As $13 \leq m \leq 23$ were found in experiments, we choose the most typical structure with $m = 17$ in this study (Fig. 2a). Unlike the highly symmetrical flat layer in lizardite, the wavy layered structure and the polarity reversion of the Si-O tetrahedral sheets generated 3 different ring structures, i.e. ordinary 6-membered rings (6R) of tetrahedra as also seen in lizardite and tremolite, and the presence of 4- and 8-membered rings (4R and 8R) at the position where the tetrahedral sheets reverse.

Since noble gas atoms incorporate interstitially in the mineral lattice, the 4R site is found to be the most energetic unfavorable compared to 6R and 8R sites as larger ring structures provide more interstitial spaces. The calculation shows that the structural energy when He on 4R site is ~ 110 kJ/mol higher than on 6R or 8R sites, hence 4R sites are rarely occupied by noble gas atoms and have negligible influence on the overall diffusion. The 6Rs are also meta-stable incorporation sites for noble gases as they have slightly higher incorporation energies than 8R. Strictly speaking, every 6R site in the antigorite unit cell is different due to minor differences in atomic environment.

However, static energetic calculations indicate that the energy differences between the different 6R sites are very small. For instance, the lowest energy 6R site for He is the S3, while the highest is the S2 site (Fig. 2), but their energy difference ($E^{\text{He-S2}} - E^{\text{He-S3}}$) is less than 0.8 kJ/mol (~ 7 meV). Compared to the energy barrier of He diffusion from S2 to S3 ($E_a^{\text{He-S2-S3}}$ = 111.9 kJ/mol), we considered the differences among 6R sites to have very limited effect on diffusion, and all the 6R sites are treated as identical in our calculations. The 8R is the incorporation site with the lowest energy for noble gases (S1 site in Fig. 2). The energy difference between 8R and 6R increases with heavier noble gas, as $E^{\text{He-S1}} - E^{\text{He-S2}}$ = -6.8 kJ/mol, $E^{\text{Ne-S1}} - E^{\text{Ne-S2}}$ = -14.5 kJ/mol, $E^{\text{Ar-S1}} - E^{\text{Ar-S2}}$ = -57.9 kJ/mol, $E^{\text{Kr-S1}} - E^{\text{Kr-S2}}$ = -87.8 kJ/mol and $E^{\text{Xe-S1}} - E^{\text{Xe-S2}}$ = -138.0 kJ/mol, thus 8R site is more retentive than other incorporation sites, especially for the heavy noble gases.

Diffusion in antigorite is very similar to that in lizardite, with inter-layer (in *a, b* directions) diffusion dominant, while the intra-layer (in *c* direction) diffusion is formidable due to the close-packed octahedral sheet. Taking S1-S2 path as the 8R-6R diffusion process and S2-S3 represents the diffusion among 6Rs, the diffusion in *a,b* direction is constrained by the process with the higher energy barrier, which in most cases is the S1-S2 path, except for Ne (Table 2).

3.3 Noble gas diffusion in tremolite

Tremolite with the ideal formula of $Ca_2Mg_5Si_8O_{22}(OH)_2$ is composed of repeating double chains of silica tetrahedra that run parallel to the c-axis. Fig. 3 shows structural schematics of tremolite viewed from different angles. The large ring-sites, also called

A-sites labeled within the schematics, are typically vacant but can be occupied by other elements, including Na, K, F and Cl. These A-sites form channels that are effective conduits for atomic incorporation and diffusion.

The diffusion in tremolite is also anisotropic, and the activation energies are similar to those in lizardite since the diffusion in the channel can be analogous to the inter-layer diffusion in lizardite. The other direction for diffusion in tremolite is different, and the atom has to jump from one channel to another as shown in Fig. 3b. This process is easier to achieve than in lizardite and antigorite due to the break in the close-packed octahedral sheets in tremolite. However, even though the energy barrier of this path is only a half of the energy barrier to go through the octahedral sheet in lizardite, it is still much higher than diffusion within the channel (for instance 189.1 kJ/mol versus 93.6 for He respectively),, and thus it may only happen if the channel is blocked by other impurity atoms.

As far as we know, there are only a few studies on noble gas diffusion in amphiboles. Jackson et al. (2016) investigated He and Ne diffusion in amphibole minerals with different chemical compositions and A-site occupancy states. They reported activation energies of 98.8 ~ 123.6 kJ/mol for He and 132.2 ~ 181.5 kJ/mol for Ne. Our calculation results are 93.6 kJ/mol for He and 158.2 kJ/mol for Ne, and thus can be considered as in good agreement with their experiment. However, the calculated activation energy for Ne diffusion is generally higher (Fig. 5), which could be due to that fact that we use the ideal chemical composition for tremolite in the calculation and all A-sites are unoccupied. Besides, experiments also show potentially higher activation energies for

Ne at high temperatures (Jackson et al. 2016). For Ar, an activation energy of 268.2 ± 7.1 kJ/mol in hornblende has been reported by Harrison (1982) and similar result of ~250 kJ/mol reported by Baldwin et al. (1990). Our theoretical result is 266.3 kJ/mol, which is also in very good consistent with the experiment (Fig. 4c).

For better comparison with experiments, the effect of different mineral chemical compositions, and more importantly the influence of occupied A-sites on diffusion have to be considered. We have, therefore, performed further calculations of He, Ne and Ar diffusion in pargasite, where all the A-sites in pargasite are taken by Na^+ cations. The diffusion activation energies are found to increase relative to tremolite for all noble gases (Fig. 5), e.g. E_a(He) increases from 93.6 to 128.0 kJ/mol, E_a(Ne) increases from 158.2 to 195.9 kJ/mol and E_a(Ar) increases from 266.3 to 319.4 kJ/mol. This is consistent with the experiment results from Jackson et al. (2016), where they found higher activation energies in amphiboles with more occupied A-sites. Also, the specific chemical composition of the mineral seems to have little effect on diffusion according to the data from Jackson et al. (2016), which is readily comprehensible given the inert nature of the noble gases. The occupied ring structure in other minerals may also inhibit noble gas diffusion, but we can expect this blockage is likely to be weaker in lizardite and antigorite as there are other optional paths for a noble gas to navigate around an occupied ring site.

4. Discussion

4.1 More comparison with experiments

Despite the direct comparison with experimental values, there are other studies that can

provide indirect information regarding noble gas diffusion. In the solubility experiments of noble gases in serpentinite minerals (Jackson et al., 2015; Krantz et al., 2019), the adsorption of noble gases into the mineral samples is controlled by the diffusion process, and the concentration-depth profile of the noble gases near the mineral-gas interfaces should be an analog to a 1-D diffusion profile. However, these experiments resulted in nearly constant concentrations from a few microns up to ~ 30 um near the mineral surface under the heating of moderate temperatures (300 ~ 350 °C) and duration of dozens of hours (< 48h). A simple estimation can be made that Dt/x^2 has to be ~ 1 to achieve this concentration profiles, where D is the diffusivity, t is the time and x is the diffusion depth. Assuming heating temperature of 350 °C and duration time t = 48h, and using $D = 1.5 \times 10^{-36}$ m^2/s for Ar in antigorite according to our calculations, the diffusion depth x is only 5×10^{-16} m which is physically unrealistic. To diffuse into the depth of 30 um, the diffusivity of the noble gas must be on the scale of 10^{-15} m^2/s and the corresponding activation energy should be less than ~ 100 kJ/mol. This extremely low activation energy is possibly if fast diffusion paths (Watson and Baxter, 2007) exist in the samples other than bulk lattice diffusion. For instance, Burnard et al. (2015) reported Ar lattice and interface diffusion in olivine and found a lattice diffusion activation energy of 338 ~ 445 kJ/mol that is also comparable to our calculation result here. However, the grain boundary diffusion activation energies in the same experiment are only 23 ~ 114 kJ/mol, and grain boundary diffusion dominates the diffusion process at low temperatures. Nevertheless, even though the diffusion of noble gases into the mineral lattices is very slow especially for Ar, Kr and Xe, their

incorporation into natural samples can be occur during mineral metamorphization, and therefore diffusion would not have significant effect on the initial budget of noble gases in the subduction system.

4.2 Retention of noble gases during the subduction

According to closure temperatures (T_c) given in Table 2, lizardite and tremolite have similar retentive properties for all the noble gases, while the diffusive activation energies are generally slightly higher in lizardite except for He. For all the minerals studied, the *Tc* of He is too low to be trapped in lizardite and tremolite even at ambient temperatures, or under low hydrothermal conditions in antigorite. However, things become more subtle for Ne as the *Tc* of Ne in lizardite is close to its transition temperature from lizardite to antigorite. The stable temperature for lizardite at 0 GPa is about 300 ~ 320 °C, and it decreases with increasing pressure where it is 280 ~ 300 °C at 1 GPa (Evans, 2004). Since the retention of the noble gases, especially for Ne, is very sensitive to any changes of the diffusion, the pressure effects on noble gas diffusions are found to be nontrivial (Table 3). For instance, the E_a*(Ne-lizardite)* increases to 190.1 kJ/mol at 1 GPa from 157.3 kJ/mol at ambient pressure, and the closure temperature increases substantially to 290 °C from 195 °C. In this case, original Ne in lizardite might be inherited by antigorite after lizardite-antigorite phase transition and become entrained to much deeper depths.

In contrast to the concept of closure temperature which represents the end of diffusive loss of elements in minerals in a gradually cooling environment, the subduction process is accompanied by temperature increase. Using the same parameters in T_c calculation,

but changing the cooling environment to a gradually heating one, Cherniak et al. (2007, 2015) concluded that ~ 40% of any diffusant will be diffusively lost when the temperature reached T_c. Since our interests are in noble gas retentions in minerals during subduction heating, we adopted the calculation opposite to the closing temperature according to Watson and Cherniak (2013):

$$T_{rt\%}(K) = \frac{0.457 \cdot (E_a / R)}{\chi_h + \log[\frac{E_a \cdot D_0}{R \cdot a^2 \cdot dT / dt}]} \qquad (4)$$

where $T_{rt\%}$ (in K) is the temperature at which the fraction (rt%) of diffusant remained in the mineral, E_a is the activation energy in J/mol, D_0 is the pre-factor of Arrhenius diffusion equation in m^2/s, dT/dt is the linear heating rate in K/s, R is the gas constant and a is the grain radius in meters. χ_h is a constant corresponding to different retention fractions, e.g. 4.751 for 99.9% retention and -0.785 for 50% retention.

Fig. 6 shows the fraction of noble gases remaining in the minerals during heating from subduction. As expected, ~40 % of noble gases will already be lost when the temperature reached their *Tc*, suggesting that the closure temperature alone cannot provide sufficient information regarding the 'openness' of a system to diffusive loss when heated. To understand noble gas recycling, it is critical to know how much of them will be released or retained when the carrier minerals break down. At the transition temperature of 300 °C for lizardite to antigorite , the remaining noble gases in lizardite is composed of 0% He, 0% ~ 80% Ne depending on the grain size and 100% for Ar, Kr and Xe (Fig. 6a). For antigorite, as its dehydration temperature is ~ 650 °C at 3 GPa, the only change in the residual noble gases is the remaining fraction of Ne which varies

from 0% ~ 70% (Fig. 6b), slightly less retentive than when lizardite tranforms. Therefore, the serpentinised oceanic lithosphere tends to carry heavy noble gases (Ar, Kr and Xe) with no elemental fractionation among them. This is consistent that the Ar-Kr-Xe characteristic of the MORB mantle indicates a mixing with sea-water component (Holland and Ballentine, 2006; Kendrick et al., 2011; Smye et al., 2017; Krantz et al., 2019). The partial retention of Ne in the serpentinite is also in agreement with the Ne isotope characteristics in exhumed serpentinites (Kendrick et al., 2018) and might be able to explain the possibility that ~ 30% of mantle Ne is atmospheric (Holland and Ballentine, 2006; Jackson et al., 2015; Williams and Mukhopadhyay, 2019).

Tremolite is stable to high temperature (> 850 °C) but at relatively low pressure (< 3 GPa) (e.g. Debret et al., 2016), hence its dehydration is controlled by the depth where it reaches 3 GPa. The temperature of typical oceanic crust at this depth is between 300 ~ 680 °C, from the cold part of oceanic MOHO isolated from the heating to the hot extrusive crust heating by the contact with the overlying mantle wedge. Within this temperature range, most of the Ne will be lost except that in minerals with relatively large grain sizes (at least a few dozens of microns) and located in the coldest part of the slabs. Ar and Kr will experience different extractions. Throughout most of the subducted crust, Ar will be largely preserved. Kr begins to degas from 570 °C, and only a small fraction of Kr will lost at 680 °C finally. The overlap of the temperature ranges for noble gases to escape from tremolite suggests that when tremolite dehydrates, the different parts of the subducted crust have progressively fractionated elemental ratios, with more enrichment in heavier noble gases from the uppermost to the bottom, e.g. the

Ne:Ar:Kr:Xe is 0.8:1:1:1 at 300 °C and 0:0.9:1:1 at 680 °C.

It is also worth noting that the retention calculation performed here is a simplified model that only focuses on the retention of noble gases in the hydrous minerals, and once the noble gases have diffused out of the mineral lattice they are assumed to be lost from the subduction system. However, subducting slabs are evolving systems that are accompanied with continuous mineral dehydrations and hydrations. Noble gases lost from the hydrous minerals will probably go along with the released fluids and participate the hydration of other minerals again. Moreover, the dehydration of hydrous minerals is not necessarily a catastrophic event to release all the incorporated noble gases if it does not involves total breakdown of the original minerals to form new minerals. For instance, tremolite decomposes into diopside + enstatite + silica + water under heating, and this transformation is possibly accomplished via the rearrangement of its original lattice structure (Johnson and Fegley, 2003), and thus the noble gas within it will likely still be carried by the next-phase minerals (Kendrick et al., 2018).

5. Conclusions

The diffusion of noble gases (He, Ne, Ar, Kr and Xe) in lizardite, antigorite and tremolite have been calculated based on first-principles calculation in this study. In all minerals, diffusion follows the same pattern that $D_{He} > D_{Ne} > D_{Ar} > D_{Kr} > D_{Xe}$. The theoretical results are in excellent agreement with available experimental measurements made in amphiboles, and thus proves the validity of diffusion mechanism and theory foundation adopted in our calculation. The common ring sites constructed by the Si-O tetrahedra in the hydrous minerals provide vacant spaces to

incorporate the noble gas atoms, and the different atomic structure of the ring sites causes variable diffusive activation energies. As the size of the 8R ring structure in the antigorite is the largest, it has a strong trapping effect on the noble gas atoms. As a result, antigorite is the most retentive mineral for all noble gases such that some Ne remains even at ~ 650 °C, beyond the stability field of the antigorite. In contrast, Ne in lizardite and tremolite will be completely removed when T increases to 400 °C. This indicate that serpentinite, as major volatile-element-bearing phases in the hydrous altered oceanic lithosphere, may serve as carriers to transport large quantities of atmospheric noble gas with unfractionated Ar-Kr-Xe to potentially mix with the depleted degassed mantle. Tremolite, which is more important in altered oceanic crust, has variable abilities in keeping its noble gases due to the large temperature variations during subduction, e.g. tremolite in the cold (deep) part of the crust can retain unfractionated Ar-Kr-Xe as with antigorite, but in hot (extrusive part) zones only part of the Ar and over ~ 90% of the Xe can remain in the tremolite. The effect of delivering atmospheric noble gases by subduction may play a significant role in shaping the mantle noble gas characteristic over geological time. The elemental fractionation of noble gases along with subduction may also have left some traces in mantle noble gas isotopes. The exact details of how noble gases are recycled into the deeper mantle will require further study. In particular we will need to understand the fate of noble gas-rich fluids after devolatilization. The dehydration released fluids can either react and impart a noble gas signature into the mantle wedge or interact with the subducting slab again, and some of the noble gases will eventually reach to deep mantle. Other minerals can

be found in subduction systems might also play roles in delivering noble gases to deep Earth, as even nominally anhydrous minerals formed by the breakdown of hydrous minerals are much more enriched in sea-water derived noble gases than their counterparts in the ordinary mantle. Nevertheless, our work shows that diffusive loss must be considered in this process.

Acknowledgements

We acknowledge the supports by National Natural Science Foundation of China to K.W. (41602032) and to X.L. (41425009). This work was performed using the computing facilities at the High Performance Computing Center (HPCC) of Nanjing University and Tianhe-2 at the National Supercomputer Center of China (NSCC) in Guangzhou.

Reference

Amiguet E., Van De Moortèle B., Cordier P., Hilairet N. and Reynard B. (2014) Deformation mechanisms and rheology of serpentines in experiments and in nature. *J. Geophys. Res. Solid Earth*. **119**, 4640–4655.

Baldwin S. L., Harrison T. M. and Gerald J. D. F. (1990) Diffusion of ^{40}Ar in metamorphic hornblende. *Contrib. to Mineral. Petrol.* **105**, 691–703.

Ballentine C. J. and Holland G. (2008) What CO_2 well gases tell us about the origin of noble gases in the mantle and their relationship to the atmosphere. *Philos. Trans. R. Soc. A Math. Phys. Eng. Sci.* **366**, 4183–4203.

Baxter E. F. (2010) Diffusion of noble gases in minerals. *Rev. Mineral. Geochemistry*. **72**, 509-557.

Blöchl P. E. (1994) Projector augmented-wave method. *Phys. Rev. B* **50**, 17953–17979.

Bostock M. G., Hyndman R. D., Rondenay S. and Peacock S. M. (2002) An inverted continental moho and serpentinization of the forearc mantle. *Nature* **417**, 536–538.

Burnard P. G., Demouchy S., Delon R., Arnaud N. O., Marrocchi Y., Cordier P. and Addad A. (2015) The role of grain boundaries in the storage and transport of noble gases in the mantle. *Earth Planet. Sci. Lett.* **430**, 260–270.

Cai C., Wiens D. A., Shen W. and Eimer M. (2018) Water input into the Mariana subduction zone estimated from ocean-bottom seismic data. *Nature* **563**, 389–392.

Capitani G. and Mellini M. (2004) The modulated crystal structure of antigorite: The m = 17 polysome. *Am. Mineral.* **89**, 147–158.

Cherniak D. J., Amidon W., Hobbs D. and Watson E. B. (2015) Diffusion of helium in carbonates: Effects of mineral structure and composition. *Geochim. Cosmochim. Acta* **165**, 449–465.

Dallai L., Broadley M. W., Ballentine C. J. and Burgess R. (2016) Sedimentary halogens and noble gases within Western Antarctic xenoliths : Implications of extensive volatile recycling to the sub continental lithospheric mantle. *Geochim. Cosmochim. Acta* **176**, 139–156.

Debret B., Koga K. T., Cattani F., Nicollet C., Van den Bleeken G. and Schwartz S. (2016) Volatile (Li, B, F and Cl) mobility during amphibole breakdown in subduction zones. *Lithos* **244**, 165–181.

Deschamps F., Guillot S., Godard M., Chauvel C., Andreani M. and Hattori K. (2010) In situ characterization of serpentinites from forearc mantle wedges: Timing of serpentinization and behavior of fluid-mobile elements in subduction zones. *Chem. Geol.* **269**, 262–277.

Dodson M. H. (1973) Closure temperature in cooling geochronological and petrological systems. *Contrib. to Mineral. Petrol.* **40**, 259–274.

Evans B. W. (2004) The Serpentinite Multisystem Revisited: Chrysotile Is Metastable. *Int. Geol. Rev.* **46**, 479–506.

Farley K. A., Maier-Reimer E., Schlosser P. and Broecker W. S. (1995) Constraints on mantle 3He fluxes and deep-sea circulation from an oceanic general circulation model. *J. Geophys. Res.* **100**, 3829–3839.

Ghaderi N., Zhang H. and Sun T. (2015) Relative stability and contrasting elastic properties of serpentine polymorphs from first-principles calculations. *J. Geophys. Res. Solid Earth*

120, 4831–4842.

Graham D. W. (2002) Noble Gas Isotope Geochemistry of Mid-Ocean Ridge and Ocean Island Basalts: Characterization of Mantle Source Reservoirs. *Rev. Mineral. Geochemistry* **47**, 247–317.

Harrison T. M. (1982) Diffusion of ^{40}Ar in hornblende. *Contrib. to Mineral. Petrol.* **78**, 324–331.

Holland G. and Ballentine C. J. (2006) Seawater subduction controls the heavy noble gas composition of the mantle. *Nature* **441**, 186–191.

Jackson C. R. M., Parman S. W., Kelley S. P. and Cooper R. F. (2015) Light noble gas dissolution into ring structure-bearing materials and lattice influences on noble gas recycling. *Geochim. Cosmochim. Acta* **159**, 1–15.

Jackson C. R. M., Parman S. W., Kelley S. P. and Cooper R. F. (2013) Noble gas transport into the mantle facilitated by high solubility in amphibole. *Nat. Geosci.* **6**, 562–565.

Jackson C. R. M., Shuster D. L., Parman S. W. and Smye A. J. (2016) Noble gas diffusivity hindered by low energy sites in amphibole. *Geochim. Cosmochim. Acta* **172**, 65–75.

Johnson N. M. and Fegley B. (2003) Tremolite decomposition on Venus II. Products, kinetics, and mechanism. *Icarus* **164**, 317–333.

Kendrick M. A., Honda M., Pettke T., Scambelluri M., Phillips D. and Giuliani A. (2013) Subduction zone fluxes of halogens and noble gases in seafloor and forearc serpentinites. *Earth Planet. Sci. Lett.* **365**, 86–96.

Kendrick M. A., Scambelluri M., Hermann J. and Padrón-Navarta J. A. (2018) Halogens and noble gases in serpentinites and secondary peridotites: Implications for seawater subduction and the origin of mantle neon. *Geochim. Cosmochim. Acta*. **235**, 285-304.

Kendrick M. a., Scambelluri M., Honda M. and Phillips D. (2011) High abundances of noble gas and chlorine delivered to the mantle by serpentinite subduction. *Nat. Geosci.* **4**, 807–812.

Kobayashi M., Sumino H., Nagao K., Ishimaru S., Arai S., Yoshikawa M., Kawamoto T., Kumagai Y., Kobayashi T., Burgess R. and Ballentine C. J. (2017) Slab-derived halogens and noble gases illuminate closed system processes controlling volatile element transport into the mantle wedge. *Earth Planet. Sci. Lett.* **457**, 106–116.

Krantz J. A., Parman S. W. and Kelley S. P. (2019) Recycling of heavy noble gases by subduction of serpentinite. *Earth Planet. Sci. Lett.* **521**, 120–127.

Kresse G. (1999) From ultrasoft pseudopotentials to the projector augmented-wave method. *Phys. Rev. B* **59**, 1758–1775.

Kresse G. and Furthmüller J. (1996) Efficiency of ab-initio total energy calculations for metals and semiconductors using a plane-wave basis set. *Comput. Mater. Sci.* **6**, 15–50.

Kresse G. and Hafner J. (1993) Ab initio molecular dynamics for liquid metals. *Phys. Rev. B* **47**, 558–561.

Marty B. (2012) The origins and concentrations of water, carbon, nitrogen and noble gases on Earth. *Earth Planet. Sci. Lett.* **313–314**, 56–66.

Mellini M. and Viti C. (1994) Crystal structure of lizardite-1T from Elba, Italy. *Am. Mineral.* **79**, 1194–1198.

Momma K. and Izumi F. (2008) VESTA: A three-dimensional visualization system for electronic and structural analysis. *J. Appl. Crystallogr.* **41**, 653–658.

Monkhorst H. J. and Pack J. D. (1976) Special points for Brillouin-zone integrations. *Phys. Rev. B* **13**, 5188–5192.

Moreira M., Blusztajn J., Curtice J., Hart S., Dick H. and Kurz M. D. (2003) He and Ne isotopes in oceanic crust: implications for noble gas recycling in the mantle. *Earth Planet. Sci. Lett.* **6872**, 1–9.

Mukhopadhyay S. (2012) Early differentiation and volatile accretion recorded in deep-mantle neon and xenon. *Nature* **486**, 101–104.

Mukhopadhyay S. and Parai R. (2019) Noble Gases: A Record of Earth's Evolution and Mantle Dynamics. *Annu. Rev. Earth Planet. Sci.* **47**, 389–419.

Perdew J. P. and Wang Y. (1992) Accurate and simple analytic representation of the electron-gas correlation energy. *Phys. Rev. B* **45**, 13244–13249.

Raudsepp M., Turnock A. C., Hawthorne F. C., Sherriff B. L. and Hartman J. S. (1987) Characterization of synthetic pargasitic amphiboles (NaCa2Mg4M3+Si6Al2O22(OH,F)2; M3+ = Al, Cr, Ga, Sc, In) by infrared spectroscopy, Rietveld structure refinement, and 27Al, 29Si, and 19F MAS NMR spectroscopy. *Am. Mineral.* **72**, 580-593.

Reynard B. (2013) Serpentine in active subduction zones. *Lithos* **178**, 171–185.

Rüpke L. H., Morgan J. P., Hort M. and Connolly J. A. D. (2004) Serpentine and the subduction zone water cycle. *Earth Planet. Sci. Lett.* **223**, 17–34.

Schwartz S., Guillot S., Reynard B., Lafay R., Debret B., Nicollet C., Lanari P. and Auzende A. L. (2013) Pressure-temperature estimates of the lizardite/antigorite transition in high pressure serpentinites. *Lithos* **178**, 197–210.

Smye A. J., Jackson C. R. M., Konrad-Schmolke M., Hesse M. A., Parman S. W., Shuster D. L. and Ballentine C. J. (2017) Noble gases recycled into the mantle through cold subduction zones. *Earth Planet. Sci. Lett.* **471**, 65–73.

Staudacher T. and Allègre C. J. (1988) Recycling of oceanic crust and sediments: the noble gas subduction barrier. *Earth Planet. Sci. Lett.* **89**, 173–183.

Syracuse E. M., van Keken P. E., Abers G. A., Suetsugu D., Bina C., Inoue T., Wiens D. and Jellinek M. (2010) The global range of subduction zone thermal models. *Phys. Earth Planet. Inter.* **183**, 73–90.

Trieloff M. and Kunz J. (2005) Isotope systematics of noble gases in the Earth's mantle: possible sources of primordial isotopes and implications for mantle structure. *Phys. Earth Planet. Inter.* **148**, 13–38.

Tsuchiya J. (2013) A first-principles calculation of the elastic and vibrational anomalies of lizardite under pressure. *Am. Mineral.* **98**, 2046–2052.

Ulmer P. and Trommsdorff V. (1995) Serpentine stability to mantle depths and subduction-related magmatism. *Science.* **268**, 858–861.

Vineyard G. H. (1957) Frequency Factors and Isotope Effects in Solid State Rate Processes. *J. Phys. Chem. Solids* **3**, 121–127.

Wang K., Brodholt J. and Lu X. (2015) Helium diffusion in olivine based on first principles calculations. *Geochim. Cosmochim. Acta* **156**, 145–153.

Watson E. B. and Baxter E. F. (2007) Diffusion in solid-Earth systems. *Earth Planet. Sci. Lett.* **253**, 307-327.

Watson E. B. and Cherniak D. J. (2013) Simple equations for diffusion in response to heating. *Chem. Geol.* **335**, 93–104.

Williams C. D. and Mukhopadhyay S. (2019) Capture of nebular gases during Earth's accretion is preserved in deep-mantle neon. *Nature* **565**, 78–81.

Yang H. and Evans B. W. (1996) X-ray structure refinements of tremolite at 140 and 295 K: Crystal chemistry and petrologic implications. *Am. Mineral.* **81**, 1117–1125.

Zhang Z. G., Stixrude L. and Brodholt J. (2013) Elastic properties of MgSiO3-perovskite under lower mantle conditions and the composition of the deep Earth. *Earth Planet. Sci. Lett.* **379**, 1–12.

Zheng Y. F. (2019) Subduction zone geochemistry. *Geosci. Front.* **10**, 1223–1254.

Table 1. Calculated lattice parameters of lizardite, antigorite and Trmmolite.

		a (Å)	*b (Å)*	*c (Å)*
Lizardite	GGA[a]	5.345		7.403
	Exp[b]	5.327		7.254
	This study (GGA)	5.357		7.383
Antigorite	GGA[c]	43.84	9.33	7.38
	Exp[d]	43.505	9.251	7.263
	This study (GGA)	43.735	9.324	7.355
Trmmolite	Exp[e]	9.829	18.031	5.275
	This study (GGA)	9.980	18.185	5.331

[a](Tsuchiya, 2013); [b](Mellini and Viti, 1994); [c](Ghaderi et al., 2015); [d](Capitani and Mellini, 2004); [e](Yang and Evans, 1996)

Table 2. Calculated diffusion parameters in Eq. 1 for noble gases in lizardite, antigorite and tremolite. The diffusion activation energies (E) along the c-axis in lizardite, antigorite and the a-, b-axis in tremolite are not calculated for all noble gases because they will be too high to make any contribution to the bulk diffusion. Other parameters including v, l, D_0 are associated with E_{ab} for lizardite, higher values of $E_{s1\text{-}s2}$ and $E_{s2\text{-}s3}$ for antigorite and E_c for tremolite, respectively. The closure temperatures (T_c) are calculated assuming cylindrical mineral grains with 10 μm in radius and 100 °C/Myr cooling rate.

Lizardite	E_{ab} **(kJ/mol)**	E_c **(kJ/mol)**	v **(THz)**	l **(Å)**	$log_{10}D_0$ **(m^2/s)**	T_c **(°C)**
He	84.9	301.0	1.29	5.36	-6.255	-19.4
Ne	157.3	\	0.83	5.36	-6.447	195.0
Ar	287.5	\	4.61	5.36	-5.702	538.3
Kr	347.4	\	1.02	5.36	-6.357	737.1
Xe	414.9	\	1.51	5.36	-6.187	917.8
Antigorite	$E_{s1\text{-}s2}$/ $E_{s2\text{-}s3}$	E_c				
He	120.6/111.9	\	1.17	6.55	-6.123	81.8
Ne	193.0/267.3	\	1.19	5.36	-6.291	506.1
Ar	449.6/363.8	\	7.34	6.55	-5.326	959.6
Kr	497.9/389.8	\	5.32	6.55	-5.466	1098.4
Xe	550.0/410.1	\	6.71	6.55	-5.365	1231.0
Tremolite	E_{ab}	E_c				
He	189.1	93.6	0.89	5.33	-6.898	16.0
Ne	366.7	158.2	2.19	5.33	-6.507	199.3
Ar	\	266.3	4.26	5.33	-5.218	500.3
Kr	\	322.3	3.25	5.33	-6.336	664.6
Xe	\	385.0	7.67	5.33	-5.963	821.0

Table 3. Calculated noble gas diffusion activation energy and related closure temperatures at high pressures. Diffusion in lizardite was calculated at 1 GPa and antigorite and tremolite were calculated at 3 GPa.

	Lizardite		***Antigorite***		***Tremolite***	
	E^{1GPa} **(kJ/mol)**	T_c **(°C)**	E^{3GPa} **(kJ/mol)**	T_c **(°C)**	E^{3GPa} **(kJ/mol)**	T_c **(°C)**
He	105.2	39.6	149.6	164.8	121.6	100.1
Ne	190.1	290.1	303.0	607.6	188.2	286.4
Ar	327.1	647.3	543.3	1210.1	331.0	683.4
Kr	385.0	843.9	620.5	1427.8	387.9	850.8
Xe	464.2	1055.7	690.0	1604.5	464.2	1040.3

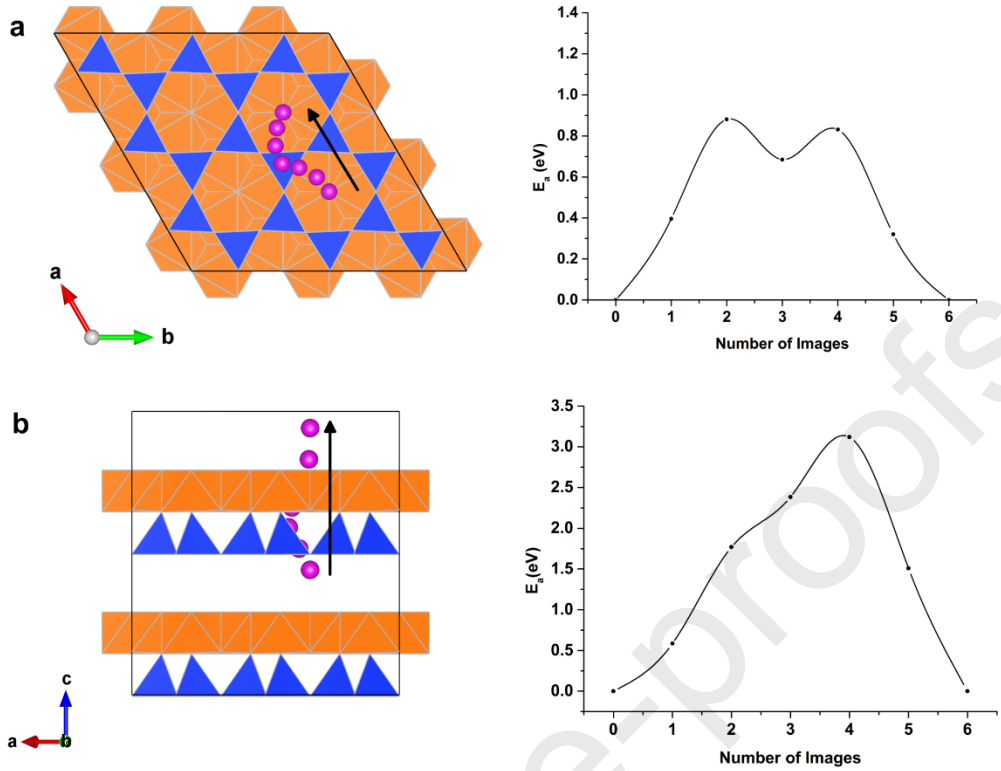

Fig.1. Schematic diffusion processes and corresponding energy profiles of He diffusing in lizardite; we use He (in purple color) as an example since other NG atoms have the same incorporation site and very similar diffusion paths. The most stable incorporation site in lizardite is at the center of the ring of Si-O tetrahedra (in blue color) viewed from c-axis, and between the layers of sheets viewed from b-axis. **a.** The diffusion path of He in the a,b-plane; **b**. The diffusion path of He along *c*-axis as atom moving across the ring and the Mg-(O-OH) octahedral sheets (in orange color). The crystal structure in this figure were drawn with polyhedral model using VESTA (Momma and Izumi, 2008).

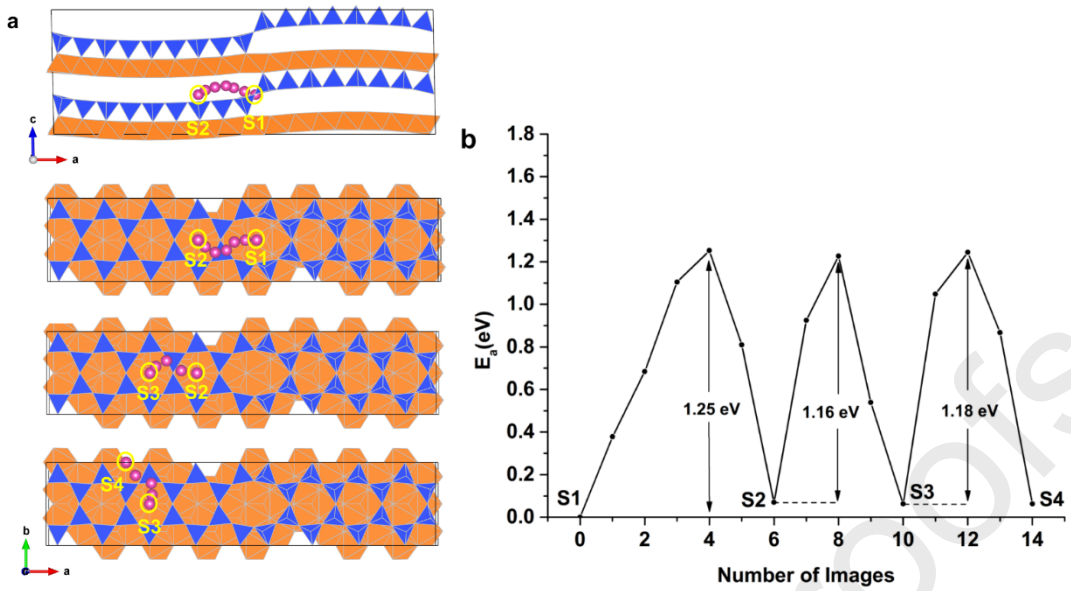

Fig. 2. **a**. Schematic diffusion processes of noble gases in antigorite. The 4 different incorporation sites are shown as S1-S4. The S1 site is the most stable as it surrounded by a large 8-membered ring. S2, S3 and S4 are sites with 6-membered rings and the differences in their incorporation energies are less than 7 meV for He and so we consider them to be equivalent. The S1 site is much more energetically favorable especially for heavier noble gases and thus it has strong trapping effect. **b**. He migration energy profile along the diffusion path of S1-S2-S3-S4.

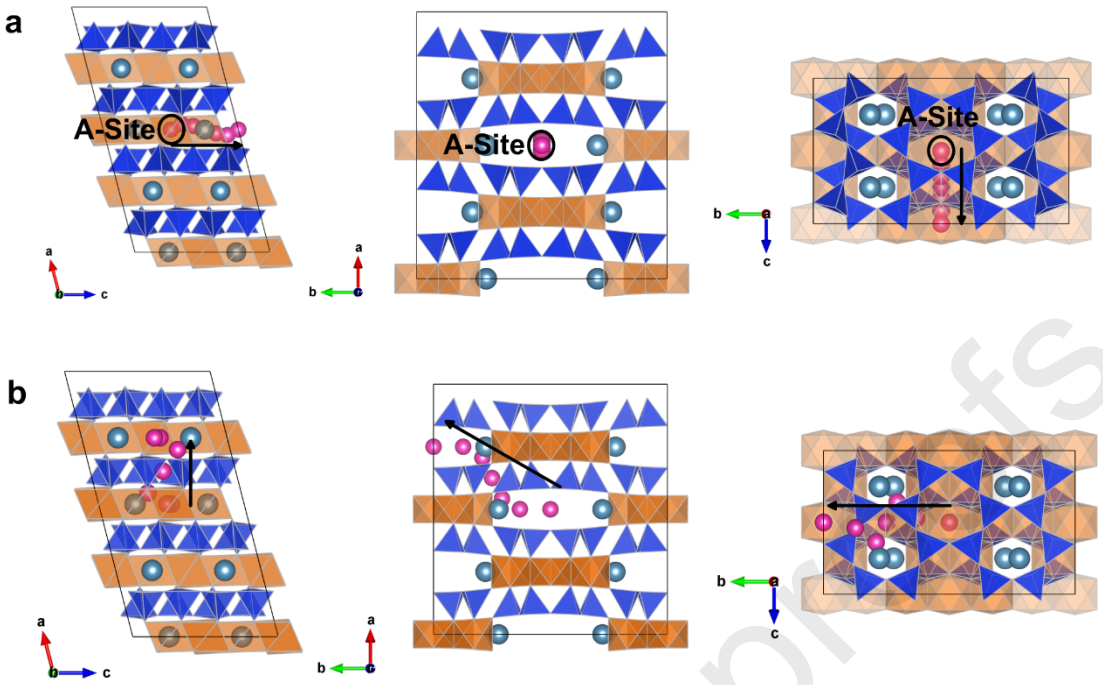

Fig. 3. Schematic diffusion of noble gases in Tremolite along the **a**. c-axis and **b**. a,b-axis from different views. We find the A-site to be the most stable incorporation position, which is inconsistent with a previous study (Jackson et al., 2013). The diffusion along the c-axis is confined within the channel formed by the vacant around the A-site, while the diffusion along a,b-axis is to go through the mismatched layered structure as shown in (b) viewed from c-axis.

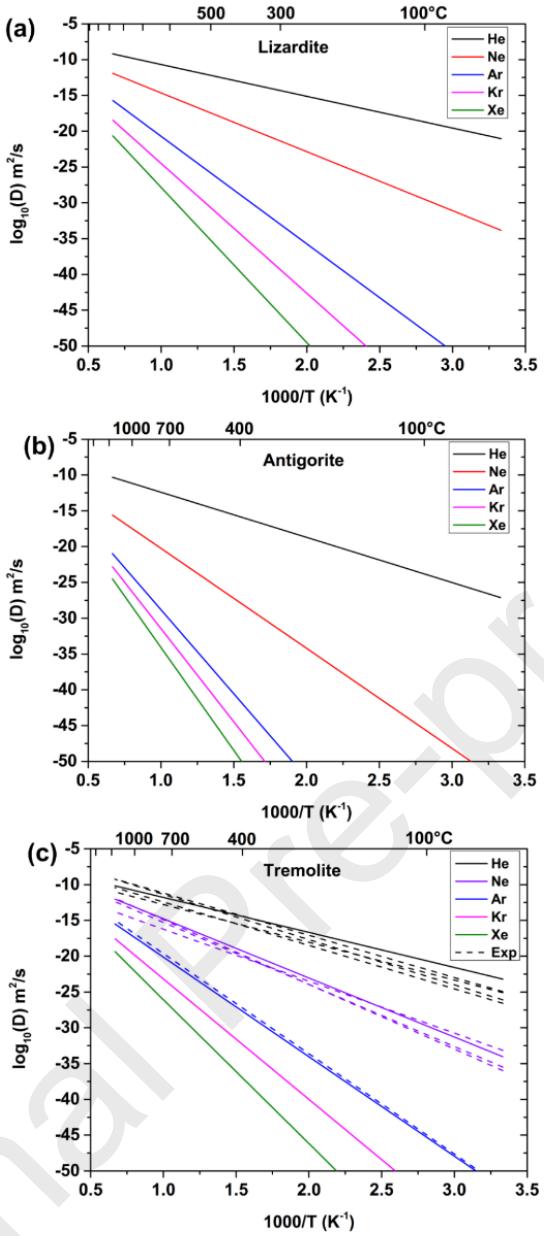

Fig. 4. Arrhenius diffusion of He, Ne, Ar, Kr and Xe in **a**. lizardite, **b**. antigorite and **c**. tremolite. Solid lines are results of our calculation and dashed lines in (c) are from previous experiments. Diffusion of He and Ne were measured in amphiboles by Jackson et al. (2016) , and Ar values were measured in hornblende by Harrison (1982).

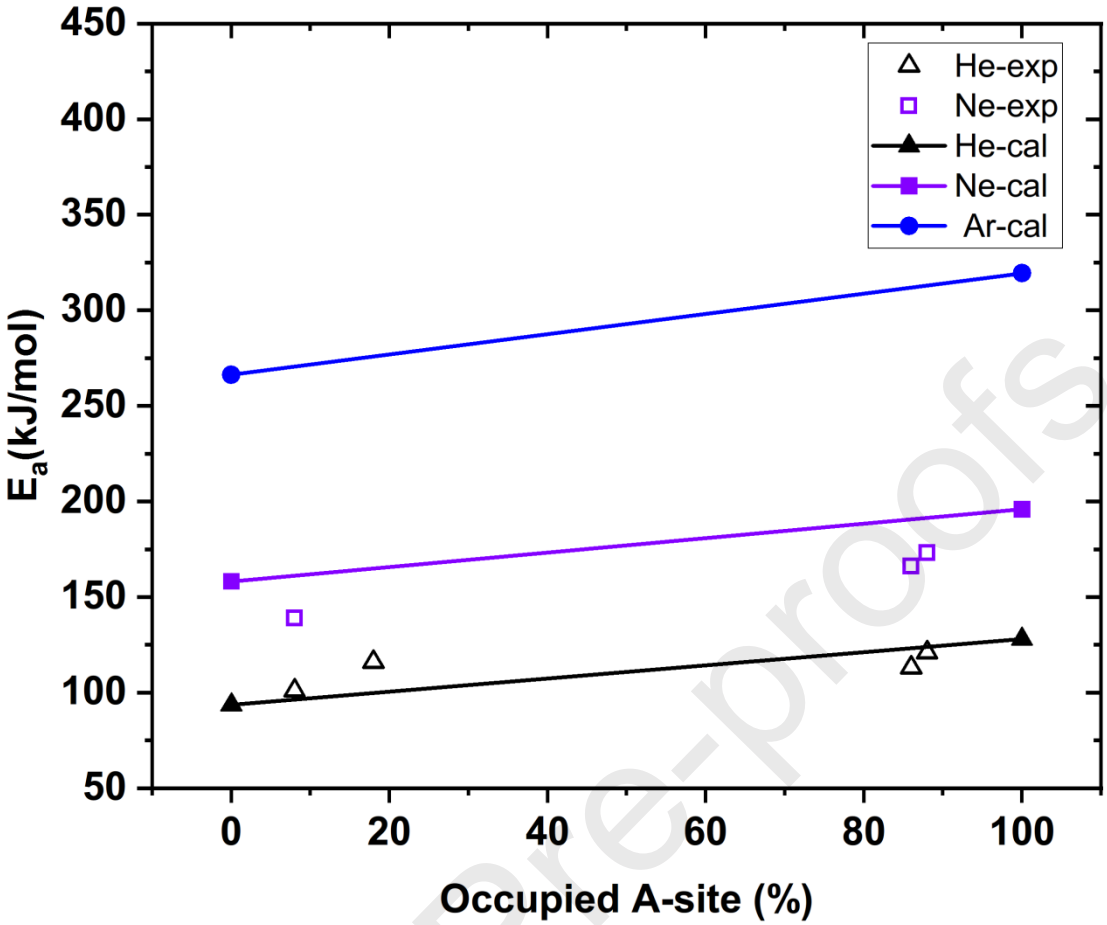

Fig. 5. The effect of concentration of occupied A-site in amphiboles on noble gas diffusion. Only none and full occupied states of A-site are investigated theoretically (filled symbols) and the previous experiment results (open symbols) cover the intermediate states (Jackson et al., 2016). Tremolite is used in our calculation to represent 0 occupied A-site structure and pargasite (with chemical formula of $NaCa_2Mg_4M^{3+}Si_6Al_2O_{22}(OF)_2$, where M^{3+} = Al, adopted from Raudsepp et al., (1987)) is used for 100% Na^+-occupied A-site state.

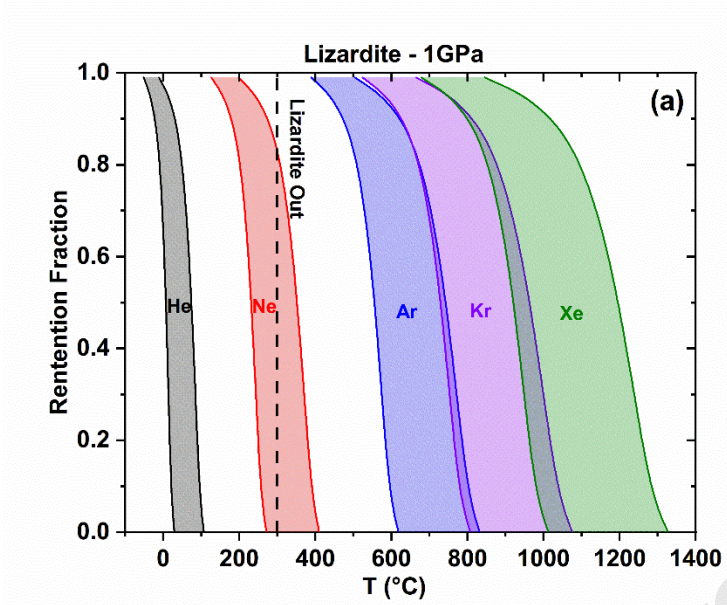

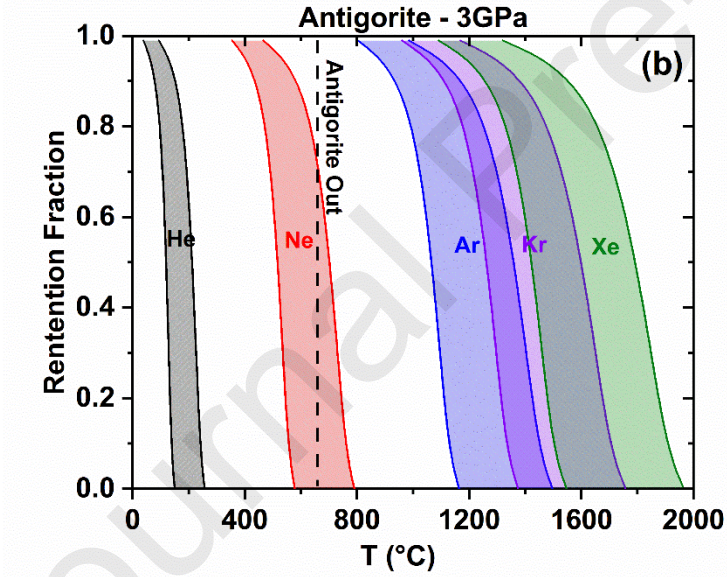

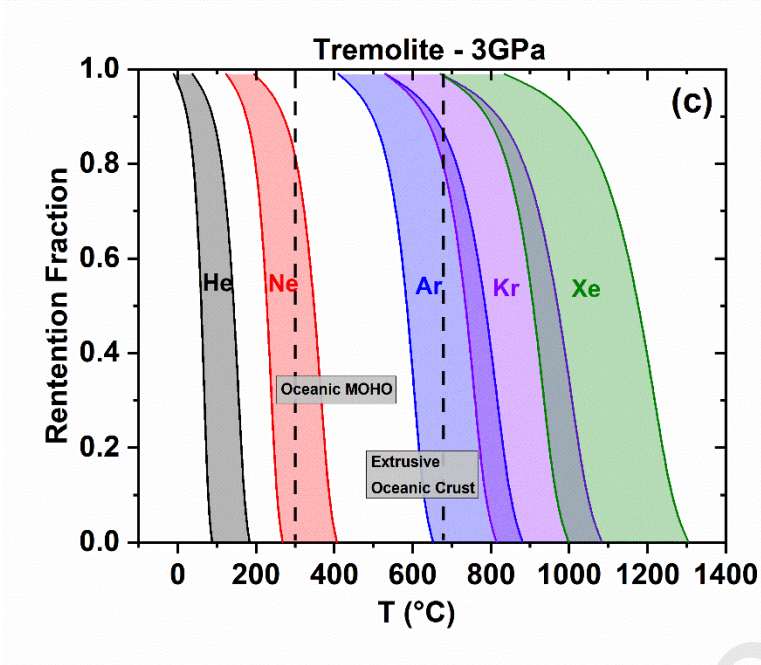

Fig. 6. The retention fractions of noble gases in **a**. Lizardite, **b**. Antigorite and **c**. Tremolite under the gradually heating environment of subduction. The minerals are assumed to be 1 μm (left boundary lines in the figures) to 100 μm (right boundary lines in the figures) in radius (e.g. Deschamps et al., 2010; Amiguet et al., 2014), and experienced a 100 °C/Myr heating rate from ambient temperature; using slower (50 °C/Myr) or faster heating rates (200 °C/Myr) from different subduction zone settings will not change the conclusion here. The concentrations of noble gases inside the minerals are initially uniformly distributed and are assumed to be lost to the environment once they diffuse out of the minerals. The dashed line in (a) and (b) represents the highest temperature of the stability field for lizardite (300 °C) and antigorite (650 °C) respectively. Tremolite can be stable at a range of temperatures and so the dashed lines show two limits of its stability at 3 GPa (oceanic MOHO of 300 °C for the lower limit and extrusive oceanic crust of 680 °C for the upper limit) used to calculate the noble gas retention fractions when tremolite dehydrates. Geotherm information is for the case of South Philippines subduction zone (Syracuse et al., 2010).

Declaration of interests

☒ The authors declare that they have no known competing financial interests or personal relationships that could have appeared to influence the work reported in this paper.

☐The authors declare the following financial interests/personal relationships which may be considered as potential competing interests: